

Supporting Information for

Synthesis, Characterization and Catalytic Activity of Ni(II) Alkyl Complexes Supported by Pyrrole-Diphosphine Ligands

Gopaladasu T. Venkanna, Swetha Tammineni, Hadi D. Arman, and Zachary J. Tonzetich*

Department of Chemistry, University of Texas at San Antonio, San Antonio, TX 78249

zachary.tonzetich@utsa.edu

Contents	Pages
Figure S1. ^1H NMR spectrum of $\text{H}(\text{P}_2^{\text{Cy}}\text{Pyr})$ (2).	S2
Figure S2. Electronic absorption spectrum of 4 in CH_2Cl_2 .	S2
Figure S3. CV of 4 in THF displaying the cathodic events observed at low potentials.	S3
Figure S4. Comparison of the cathodic events observed by CV for 3 and 4 in THF.	S3
Figure S5. CV of 4 in CH_2Cl_2 displaying the anodic events observed at higher potentials.	S4
Figure S6. Thermal ellipsoid drawing of $[\text{Ni}(\text{CH}_3)(\text{P}_2^{\text{Cy}}\text{Pyr})]$ (6).	S4
Figure S7. ^1H NMR spectrum of $[\text{Ni}(\eta^1\text{-C}_3\text{H}_5)(\text{P}_2^{\text{Cy}}\text{Pyr})]$ (14).	S5
Figure S8. ^1H NMR and IR spectra of the reaction of 5 with CO.	S5
Figure S9. ^1H NMR spectrum of $[\text{NiH}(\text{P}_2^{\text{Cy}}\text{Pyr})]$ (15).	S6
Figure S10. ^1H NMR spectrum of the reaction of 15 with CO_2 .	S6
Table S1. Crystallographic data and refinement parameters for 4 , 6 , and 7 .	S7
Table S2. Crystallographic data and refinement parameters for 10 , 11 , and 14 .	S8

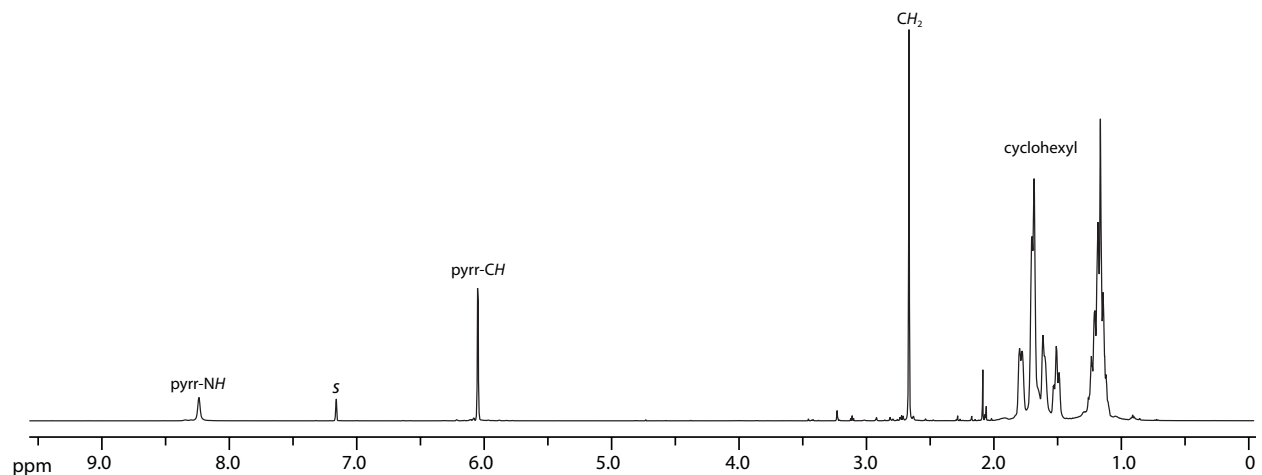


Figure S1. 500 MHz ^1H NMR spectrum of $\text{H}(\text{P}_2^{\text{Cy}}\text{Pyr})$ (2) in benzene- d_6 .

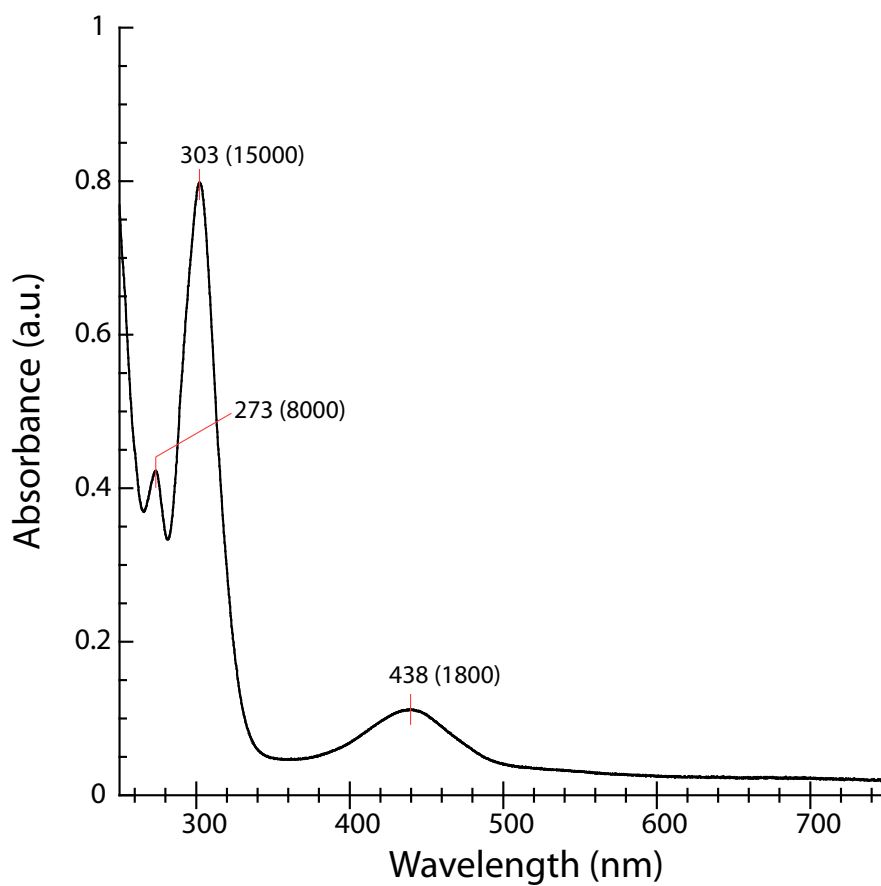


Figure S2. Electronic absorption spectrum of $[\text{NiCl}(\text{P}_2^{\text{Cy}}\text{Pyr})]$ (4) in CH_2Cl_2 (50 μM).

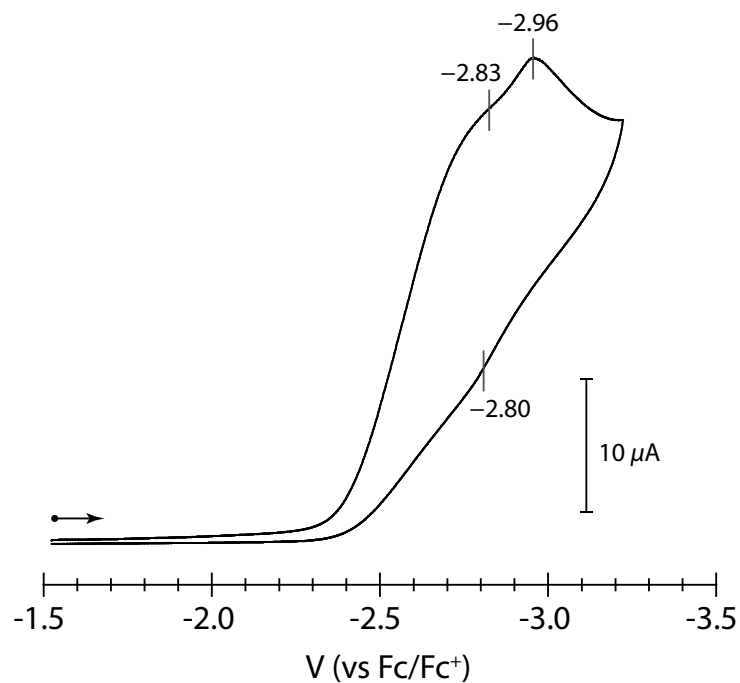


Figure S3. Cyclic voltammogram of 3 mM [NiCl(P₂^{Cy}Pyr)] (**4**) at a glassy carbon electrode in THF displaying the cathodic events observed at low potentials. Scan rate is 50 mV/s and the supporting electrolyte is 0.1 M Bu₄NPF₆.

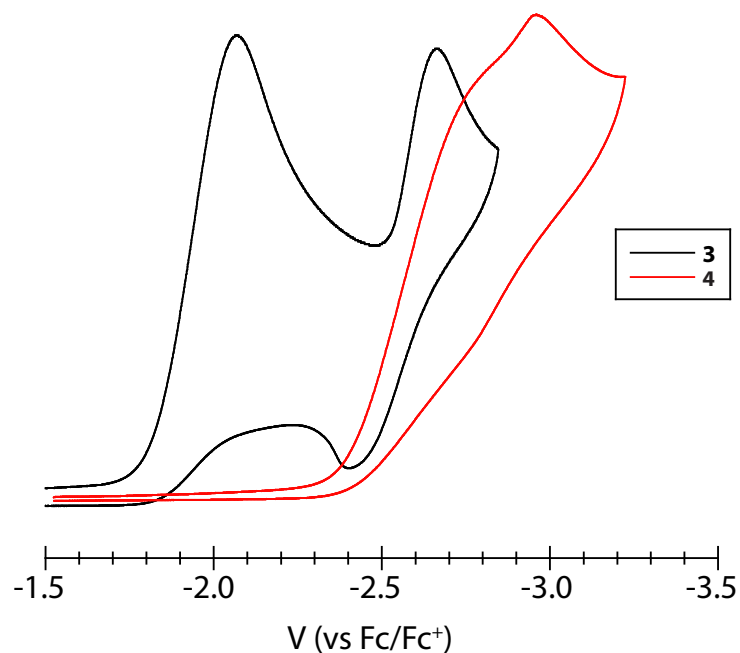


Figure S4. Comparison of the cathodic events observed for [NiCl(P₂^{Ph}Pyr)] (**3**, black) and [NiCl(P₂^{Cy}Pyr)] (**4**, red) in THF.

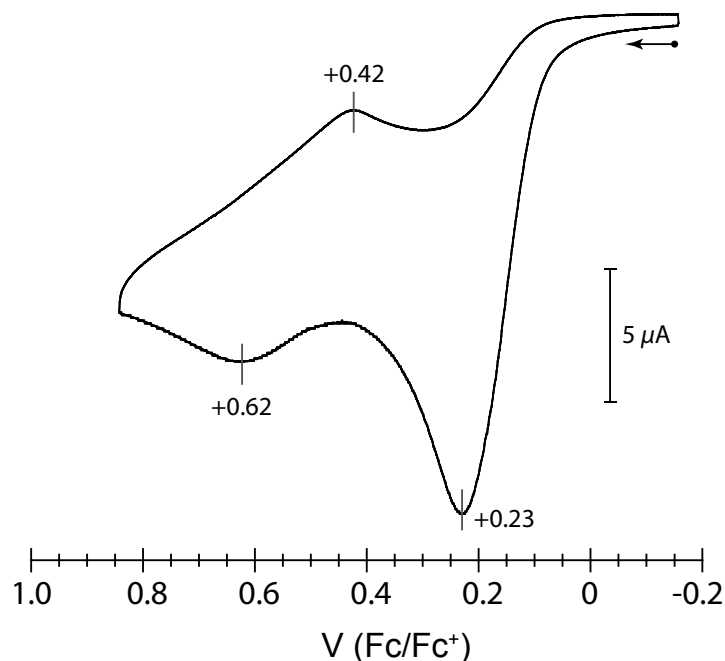


Figure S5. Cyclic voltammogram of 2 mM $[\text{NiCl}(\text{P}_2^{\text{Cy}}\text{Pyr})]$ (**4**) at a glassy carbon electrode in CH_2Cl_2 displaying the anodic events observed at higher potentials. Scan rate is 50 mV/s and the supporting electrolyte is 0.1 M Bu_4NPF_6 .

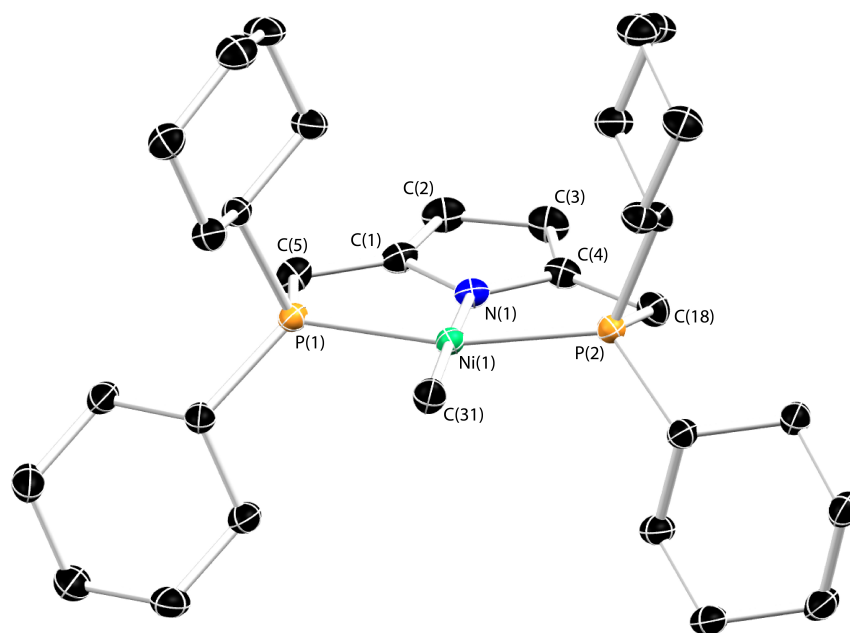


Figure S6. Thermal ellipsoid drawing (50%) of $[\text{Ni}(\text{CH}_3)(\text{P}_2^{\text{Cy}}\text{Pyr})]$ (**6**). Hydrogen atoms omitted for clarity. See Table 1 of the manuscript for selected bond lengths and angles.

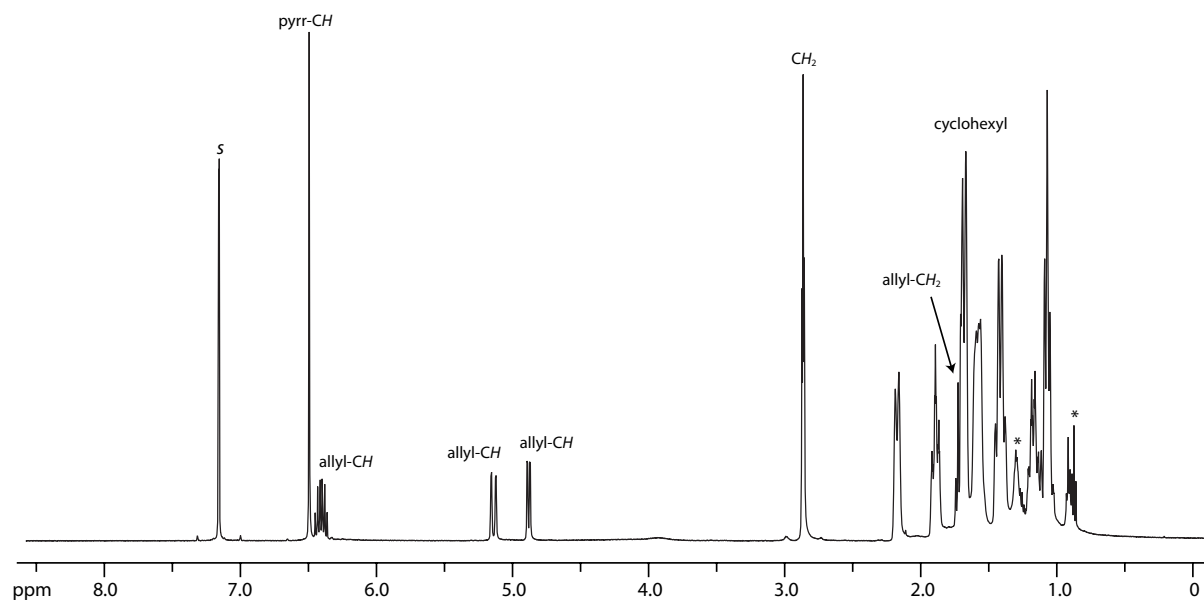


Figure S7. 500 MHz ^1H NMR spectrum of $[\text{Ni}(\eta^1\text{-C}_3\text{H}_5)(\text{P}_2^{\text{Cy}}\text{Pyr})]$ (**14**) in benzene- d_6 showing evidence for η^1 coordination of the allyl ligand in solution. Asterisks denote small amount of pentane and THF.

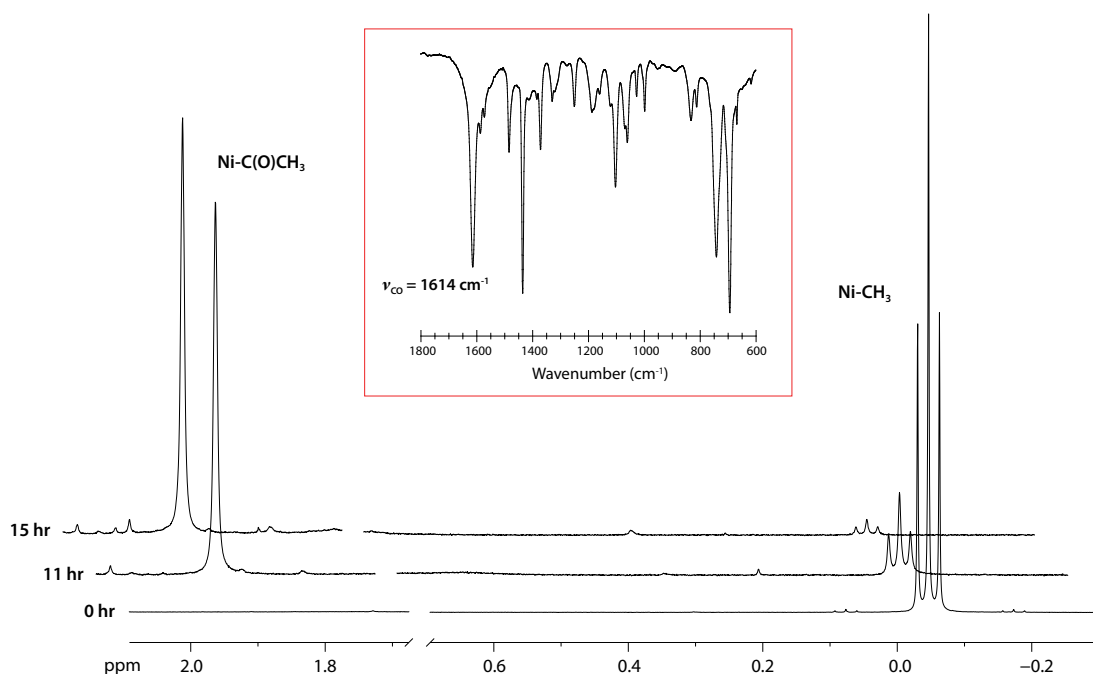


Figure S8. 500 MHz ^1H NMR spectrum of the reaction of $[\text{Ni}(\text{CH}_3)(\text{P}_2^{\text{Ph}}\text{Pyr})]$ (**5**) with excess CO (g) in benzene- d_6 showing the decrease of the methyl resonance at -0.05 ppm and growth of the acyl resonance at 1.91 ppm over 15 hrs at 50°C . Inset displays the IR spectrum (film, KBr) of the product highlighting the new carbonyl stretch at 1614 cm^{-1} .

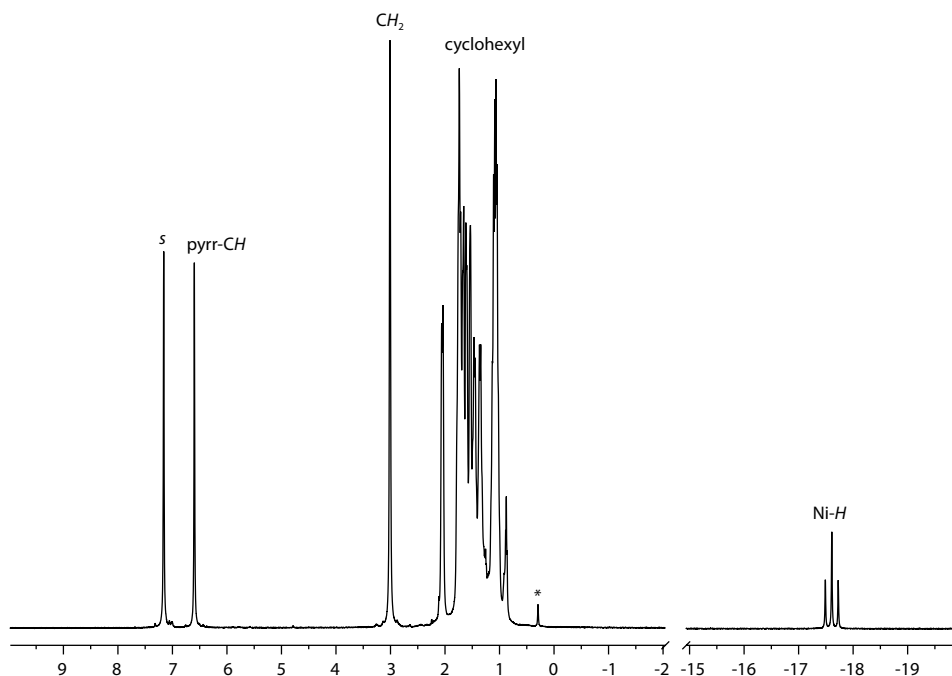


Figure S9. 500 MHz ^1H NMR spectrum of $[\text{NiH}(\text{P}_2^{\text{Cy}}\text{Pyr})]$ (**15**) in benzene- d_6 . Asterisk denotes a small amount of silicone grease.

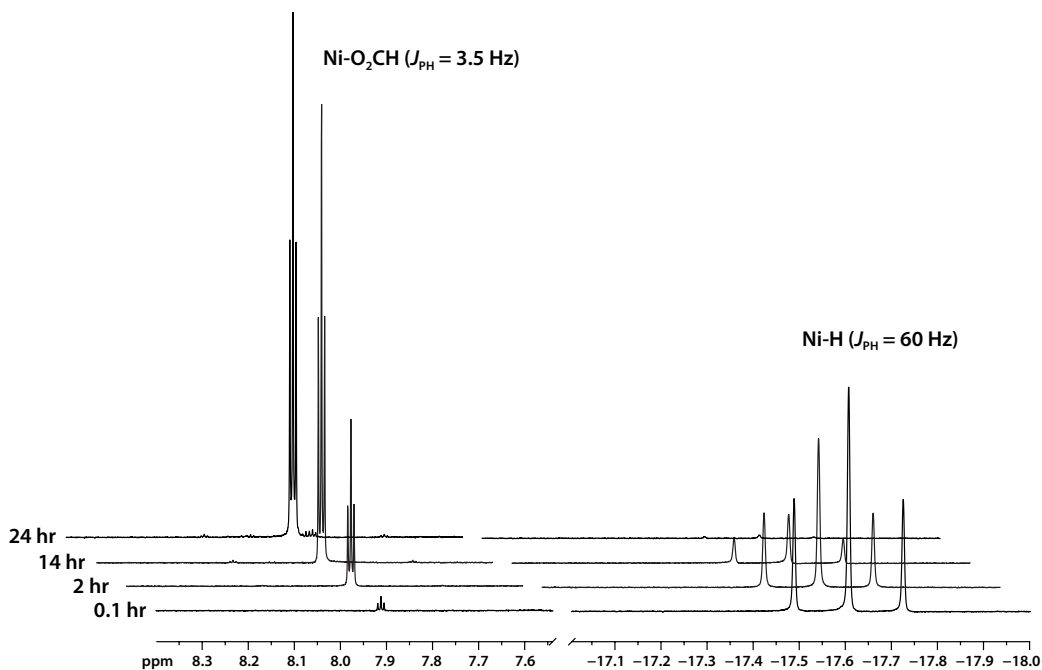


Figure S10. 500 MHz ^1H NMR spectrum of the reaction of $[\text{NiH}(\text{P}_2^{\text{Cy}}\text{Pyr})]$ (**15**) with excess CO_2 (g) in benzene- d_6 showing the decrease of the hydride resonance at -17.6 ppm and growth of the formate resonance at 7.9 ppm over 24 hrs at 23 °C.

Table S1. Crystallographic data and refinement parameters for compounds **4**, **6**, and **7**.[‡]

Compound	[NiCl(P ₂ ^{Cy} Pyr)] 4	[Ni(CH ₃)(P ₂ ^{Cy} Pyr)] 6	[Ni(C ₂ H ₅)(P ₂ ^{Ph} Pyr)] 7
Empirical formula	C ₃₀ H ₅₀ ClNNiP ₂	C ₃₁ H ₅₃ NNiP ₂	C ₃₂ H ₃₁ NNiP ₂ ·½C ₆ H ₆
Formula weight (g/mol)	580.81	560.39	589.17
Temperature (K)	98(2)	98(2)	98(2)
Crystal system, space group	Monoclinic, <i>P2₁/c</i>	Monoclinic, <i>P2₁/c</i>	Triclinic, <i>P</i> $\bar{1}$
Unit cell dimensions (Å, deg)	a = 10.220(3) b = 18.392(5) c = 15.764(4) β = 90.687(5)	a = 10.235(9) b = 18.391(2) c = 15.803(1) β = 90.638(1)	a = 10.701(1) b = 14.379(2) c = 20.688(3) α = 99.531(2) β = 90.677(1) γ = 109.668(3)
Volume (Å ³)	2962.9(1)	2975.0(3)	2948.4(7)
Z	4	4	2
Calculated density (g/cm ³)	1.302	1.251	1.324
Absorption coefficient (mm ⁻¹)	0.873	0.780	0.791
F(000)	1248	1216	1230
Crystal size (mm)	0.20 × 0.15 × 0.07	0.29 × 0.27 × 0.09	0.29 × 0.12 × 0.08
Θ range	1.99 to 26.50°	2.28 to 27.50°	2.00 to 26.00°
Limiting indices	-12 ≤ <i>h</i> ≤ 12, -23 ≤ <i>k</i> ≤ 19, -29 ≤ <i>l</i> ≤ 19	-8 ≤ <i>h</i> ≤ 13, -23 ≤ <i>k</i> ≤ 15, -20 ≤ <i>l</i> ≤ 19	-11 ≤ <i>h</i> ≤ 13, -17 ≤ <i>k</i> ≤ 15, -25 ≤ <i>l</i> ≤ 25
Reflections collected / unique	19495 / 6124 [R _{int} = 0.0492]	12035 / 6804 [R _{int} = 0.0203]	17086 / 11533 [R _{int} = 0.0264]
Completeness to Θ	99.7%	99.3%	99.4%
Absorption correction	multi-scan ABSCOR	multi-scan ABSCOR	multi-scan ABSCOR
Min. and max transmission	0.742 and 1.000	0.822 and 1.000	0.786 and 1.000
Data / restraints / parameters	6124 / 0 / 316	6804 / 0 / 316	11533 / 0 / 712
Goodness-of-fit on F ²	1.031	0.996	1.016
Final R indices [I > 2 σ (I)]	R ₁ = 0.0467, wR ₂ = 0.1066	R ₁ = 0.0357, wR ₂ = 0.0946	R ₁ = 0.0390, wR ₂ = 0.0992
R indices (all data)	R ₁ = 0.0525, wR ₂ = 0.1108	R ₁ = 0.0392, wR ₂ = 0.0993	R ₁ = 0.0435, wR ₂ = 0.1033
Largest diff. peak and hole (e ⁻ Å ⁻³)	0.678 and -0.566	0.605 and -0.569	0.783 and -0.304

[‡]Refinement method was full-matrix least-squares on F²; wavelength = 0.71073 Å. R₁ = $\sum||F_o| - |F_c|| / \sum|F_o|$; wR₂ = $\{\sum[w(F_o^2 - F_c^2)^2] / \sum[w(F_o^2)^2]\}^{1/2}$.

Table S2. Crystallographic data and refinement parameters for compounds **10**, **11** and **14**.[‡]

Compound	[Ni(CH ₂ C ₆ H ₅)(P ₂ ^{Cy} Pyr)] 10	[Ni(C ₆ H ₅)(P ₂ ^{Ph} Pyr)] 11	[Ni(η^1 -C ₃ H ₅)(P ₂ ^{Cy} Pyr)] 14
Empirical formula	C ₃₇ H ₅₇ NNiP ₂	C ₃₆ H ₃₁ NNiP ₂	C ₃₃ H ₅₅ NNiP ₂
Formula weight (g/mol)	636.49	598.27	586.44
Temperature (K)	98(2)	98(2)	98(2)
Crystal system, space group	Orthorhombic <i>Pna</i> 2 ₁	Monoclinic, <i>P</i> 2 ₁ / <i>c</i>	Monoclinic, <i>P</i> 2 ₁ / <i>c</i>
Unit cell dimensions (Å, deg)	a = 11.562(1) b = 17.618(1) c = 16.686(1)	a = 10.0884(8) b = 15.279(1) c = 19.309(2) β = 102.637(1)	a = 16.695(3) b = 15.595(3) c = 12.176(2) β = 93.919(3)
Volume (Å ³)	3399.1(5)	2904.3(4)	3163(1)
Z	4	4	4
Calculated density (g/cm ³)	1.244	1.368	1.221
Absorption coefficient (mm ⁻¹)	0.691	0.805	0.736
F(000)	1376	1248	1252
Crystal size (mm)	0.30 × 0.15 × 0.10	0.30 × 0.25 × 0.20	0.27 × 0.20 × 0.05
Θ range	2.31 to 27.50°	2.65 to 26.50°	2.61 to 27.50°
Limiting indices	-12 ≤ <i>h</i> ≤ 15, -22 ≤ <i>k</i> ≤ 22, -21 ≤ <i>l</i> ≤ 21	-12 ≤ <i>h</i> ≤ 12, -17 ≤ <i>k</i> ≤ 19, -23 ≤ <i>l</i> ≤ 24	-21 ≤ <i>h</i> ≤ 21, -20 ≤ <i>k</i> ≤ 20, -15 ≤ <i>l</i> ≤ 15
Reflections collected / unique	22437 / 7696 [R _{int} = 0.0295]	20467 / 5979 [R _{int} = 0.0203]	26998 / 7244 [R _{int} = 0.0373]
Completeness to Θ	99.4%	99.2%	99.7%
Absorption correction	multi-scan ABSCOR	multi-scan ABSCOR	multi-scan ABSCOR
Min. and max transmission	0.839 and 1.000	0.879 and 1.000	0.811 and 1.000
Data / restraints / parameters	7696 / 1 / 370	5979 / 0 / 361	7244 / 0 / 352
Goodness-of-fit on F ²	0.990	1.013	1.016
Final R indices [I > 2 σ (I)]	R ₁ = 0.0267, wR ₂ = 0.0626	R ₁ = 0.0282, wR ₂ = 0.0756	R ₁ = 0.0338, wR ₂ = 0.0835
R indices (all data)	R ₁ = 0.0273, wR ₂ = 0.0630	R ₁ = 0.0296, wR ₂ = 0.0772	R ₁ = 0.0357, wR ₂ = 0.0855
Largest diff. peak and hole (e ⁻ Å ⁻³)	0.283 and -0.213	0.343 and -0.261	0.745 and -0.261

[‡]Refinement method was full-matrix least-squares on F²; wavelength = 0.71073 Å. R₁ = $\sum||F_o| - |F_c|| / \sum|F_o|$; wR₂ = $\{\sum[w(F_o^2 - F_c^2)^2] / \sum[w(F_o^2)^2]\}^{1/2}$.